

Detection of Neovascularization in Proliferative Diabetic Retinopathy Fundus Images

Suma Gandhimathi¹ and Kavitha Pillai²

¹Department of Computer Science and Engineering, Sree Vidyanikethan Engineering College, India

²Department of Computer Science and Engineering, University College of Engineering, India

Abstract: Neovascularization is a serious visual consequence disease arising from Proliferative Diabetic Retinopathy (PDR). The condition causes progressive retinal damage in persons suffering from Diabetes mellitus, and is characterized by busted growth of abnormal blood vessels from the normal vasculature, which hampers proper blood flow into the retina because of oxygen insufficiency in retinal capillaries. The present paper aims at detecting PDR neovascularization with the help of the Adaptive Histogram Equalization technique, which enhances the green plane of the fundus image, resulting in enrichment of the details presented in the fundus image. The neovascularization blood vessels and the normal blood vessels were both segmented from the equalized image, using the Fuzzy C-means clustering technique. Marking of the neovascularization region, was achieved with a function matrix box based on a compactness classifier, which applied morphological and threshold techniques on the segmented image. Subsequently, the Feed Forward Back-propagation Neural Network interacted with extracted features (e.g., number of segments, gradient variation, mean, variance, standard deviation, contrast, correlation, entropy, energy, homogeneity, cluster shade towards the neovascularization detection region), in an attempt to achieve accurate identification. The above method was tested on images from three online datasets, as well as two hospital eye clinics. The performance of the detection technique was evaluated on these five image sources, and found to show an overall accuracy of 94.5% for sensitivity of 95.4% and of specificity 49.3% respectively, thus reiterating that the method would play a vital role in the study and analysis of Diabetic Retinopathy.

Keywords: Diabetic retinopathy, neovascularization, fuzzy C-means clustering, compactness classifier, feature extraction, neural network.

Received May 28, 2015; accepted December 27, 2015

1. Introduction

Diabetic Retinopathy (DR), the most common diabetic eye disease, occurs when prolonged hyperglycemia compels retinal blood vessels to undergo changes that progressively damage the microvascular system of that region, ultimately leading to loss of vision [3].

Statistics from the world health organization reveal that nearly 197 million people worldwide, are victims of diabetes mellitus, and that the incidence is likely to increase to 420 million by 2025 [19]. India, most unfortunately, is emerging as a potential world capital for the disease, by year 2030 [27], with the present figure of 40.9 million diabetes patients expected to rise to 69.9 million by 2025 [19]. Diabetes mellitus affects eyes, kidneys, digestion and skin. The ophthalmic abnormalities of DR are majorly classified as Non-Proliferative Diabetic Retinopathy (NPDR) and Proliferative Diabetic Retinopathy (PDR), both of which do not exhibit any early warning signs [27].

NPDR damages retinal blood vessels, causing them to leak extra fluid and small amounts of blood into the eye [4]. NPDR includes: Microaneurysms, which are small bulges in the retinal blood vessels that constantly leak tiny spots of blood. Hemorrhages, which are immensely large blood spots that drip into the retina, Exudates, which are deposits of cholesterol or other

fluids that have leaked into the retina, Macular edema, or the swelling of the macula, caused by fluid leaks from blood vessels. Macular ischemia is a condition where the macula does not receive enough blood flow, resulting in closure of small blood vessels. Many diabetic patients with mild NPDR do not get serious interruption of vision. Vision in NPDR patients gets affected usually at the end-stage of macular edema and macular ischemia [4].

PDR, on the other hand, may cause severe vision loss because it can affect both central and peripheral vision with the proliferation of new blood vessels at the back of the eye. PDR includes: Neovascularization, or closure of normal retinal blood vessels, with resultant impairment of normal blood flow to the area.

The retina responds by growing new abnormal blood vessels that do not support proper blood flow into the retina. Vitreous hemorrhage is the newly formed blood vessels bleed into the vitreous. This might impair vision if the hemorrhage happens to be very large [4]. Thus, it is evident that PDR prevents normal blood flow to the eye, with the added possibility of adversely affecting vision.

Optical Coherence Tomography (OCT), IntraVenous Fluorescein Angiography (IVFA) and Fundus photography are all used to analyze the retinal portion of the eye. OCT serves to display the structure

of the eye by providing tissue level information such as macular holes, intra-retinal layers, and so on. IVFA, used for appraising internal blood circulation of the eye, is useful for detecting DR abnormalities and age-related macular degeneration. Fundus photography provides details about the interior surface of the eye, and is useful in diagnosing DR abnormalities [5]. Until recently, fundus image was the only means of quantifying retinal morphology. The analysis includes image quality verification, segmentation of retinal structures, segmentation of abnormalities arising from DR, pigment epithelium related abnormalities, choroid related abnormalities and others [1].

The following Section is a moderately in-depth review of literature relevant to the topic of DR abnormalities. Rest of the paper is presented as section 3 that explains the implementation methodology with the results obtained, and section 4 discussion and conclusion converses about the presented work.

2. Literature Reviews

Neovascularization can be observed within the iris, choroid, vein-ocular, corneal and retinal regions of the eye. Of these, retinal neovascularization is the most serious abnormality associated with PDR [30]. Despite this fact, research in this field is not as extensive as in the area of exudates, and microaneurysms and hemorrhages.

Exudates are yellowish intra-retinal deposits, and one of the primary lesions associated with NPDR. They appear as bright patches with a variety of borders. Walter *et al.* [32] presented the Standard Contrast stretching technique for enhancement of hard exudates. Their technique identified exudates using high gray level variation, optic disc partitioning, based on morphological filtering technique, and watershed transformation from exudates.

Vimala and Mohideen [29] report enhancement of image with the use of Contrast Limited Adaptive Histogram Equalization, where segmentation of exudates takes place through the K-means clustering algorithm. These researchers extracted and fed features like color and texture as inputs into the SVM classifier which segregates exudates. Similarly, Akila and Kavitha [2] describe image enhancement with CLAHE, and segmentation of exudates by K-means clustering. Features like standard deviation, mean, energy, entropy, and homogeneity of the segmented region were fed as inputs into Random Forest Classification, which classifies exudates.

Osareh *et al.* [23] state that classification of exudates from colored retinal images were achieved using Fuzzy C-means clustering (FCM) with an artificial neural network classifier. In their research study, Thomas *et al.* [28] detected images of both Optic Disc and exudates; by applying Fuzzy logic algorithm; exudates had to be separated from the Optic

Disc.

Extensive research has been carried out to establish techniques for the detection of exudates, providing a treasure-house of information for the benefit of DR patients.

The earliest signs of DR are microaneurysms, which appear as small red dots in the retinal region. Niemeijer *et al.* [21] suggest methodology using pixel classification using k-nearest neighbour classifier for separating a combination of vasculature and red lesions from the background of the obtained image. In another study, Fleming *et al.* [11] validate initial image enhancement using contrast normalization differentiates microaneurysms from other dots present in the image, followed by watershed transformation to derive a region free from both blood vessels and other lesions. Manimala and Gokulakrishnan. [17] detects microaneurysms using FCM, and the features were extracted using Gray-level Co-Occurrence Matrix (GLCM).

An automatic pre-screen DR procedure using multiple CAD algorithms, and operated with multiple images, has been introduced in year 2009 [20]. The method successfully identifies whether DR is normal or not, using several different fusion methods. 60,000 images can be evaluated based on 15,000 examinations. Similarly, a Retinopathy Online Challenge (ROC) competition was conducted to detect microaneurysms in year 2010 [22], in which 5 different methods were compared by 5 teams of researchers, for the same set of data. The study showed that detection of microaneurysm is a difficult task, and the scheme could not achieve the desired results.

Abràmoff *et al.* [1] present an outsized survey on retinal imaging, reviews clinically relevant assessment procedures for retinal vasculature, identification of retinal lesions, etc. Furthermore, the survey also throws light on the technical challenges in fundus imagery such as diminishing and eliminating contrast due to corneal and lenticular reflections.

Research investigations related to neovascularization have been carried out extensively in the past few decades. Goatman *et al.* [14] illustrate how neovascularization vessels are classified according to their position. The paper states that new vessels have a specific appearance: they are thin in calibre, tortuous and more convoluted than normal vessels. Support Vector Machine (SVM) classifier with 15 feature parameters was used to label the vessels as normal or abnormal. Testing was done using 38 NVD images out of 71 DR images. Maximum accuracy was achieved at 84.2% sensitivity and 84.9% specificity. Hassan *et al.* [15] report identification of the region of both NVD and NVE, using compactness classifier and morphological process. A function matrix box was used to demarcate the neovascularization region from natural blood vessels.

The method was tested on images from different

databases, and achieved specificity and sensitivity results of 89.4% and 63.9%, respectively. The present study focuses on the identification of neovascularization blood vessels as an automatic process in terms of enhancement in sensitivity, specificity and accuracy.

3. Methodology for New Vessel Detection

3.1. Image Acquisition

Fundus images with several abnormalities were collected from three online databases and two hospital eye clinics covering a populace of approximately 1900 individuals. A total of 970 images with DR were included in the data set. It was found that out of the selected images, 34 from online database and 41 from hospital clinics showed definite presence of neovascularization. The image data from each source is given below.

- *IMAGERET-diaretdb0 (2006) & diaretdb1 (2007)*: The diaretdb0 database consisted of 130 color fundus images, of which 20 were normal and 110 displayed signs of DR in the form of hard exudates, soft exudates, microaneurysms and hemorrhages, and 20 images were found to exhibit neovascularization [9]. The diaretdb1 database consisted of 89 color fundus images, of which 84 showed indications of mild NPDR i.e., microaneurysms, 5 images were found with neovascularization and five normal samples [10]. Images were captured using 8 bits per color plane at 1500*1152 pixels in PNG format.
- *Messidor (2004)*: The 1200 eye fundus images were captured using 8 bits per color plane at 1440*960, 2240*1488 or 2304*1536 pixels [18]. The total number of images was divided into 4 zipped subsets each containing 100 images in TIFF format, 606 images were identified with DR and only 9 images showed neovascularization.
- *Vasan Eye care*: 76 DR fundus images were collected using Fundus camera Topcon TRC 50DX Retinal camera. 35 images showed neovascularization. Images were captured using 8 bits per color plane at 2196*1958 pixels with JPEG compressed.
- *Bejan Singh Eye Hospital*: 407 fundus images were collected using Fundus camera FF450 Plus. Of these, 94 eye fundus images showed clear indications of DR whereas only 6 images displayed neovascularization. Images were captured using 8 bits per color plane at 2240*1488 pixels with JPEG compressed.

The images obtained from three online databases and two hospital eye clinics proved to be a good representative sample for the purpose of comparison and analysis. 75 neovascularization images procured in

this manner and the reason for the low number of image selected for implementation is that only correctly defined neovascularization images declared by ground truth and by professional graders were taken into consideration. The fundus images with DR abnormalities is not present in other two well-known online fundus image databases DRIVE and STARE, and so those two databases have not been considered for implementation works.

3.2. Image Annotation

Messidor neovascularization images have been provided in an Excel file [18]. With regard to diaretdb0 database [9], ground truth documents indicate the presence of neovascularization. Two experienced professional graders (Dr.M.Pratap, Ophthalmologist of Vasan Eye Care, Nagercoil, India and Dr.S.M.BejanSingh, Ophthalmologist, Bejan Singh Eye Hospital, Nagercoil, India) annotated the abnormal images freehand in the online database samples as well as real-time clinic images. Only twisted, convoluted, busted growth pattern of vessel segments were considered abnormal by both graders.

3.3. Preprocessing

Neovascularization blood vessels are twisted and thin in nature. The busted growth pattern and uneven illumination render it extremely challenging to perform the extraction of abnormal blood vessels from the fundus image background [15] Figure 1-a.

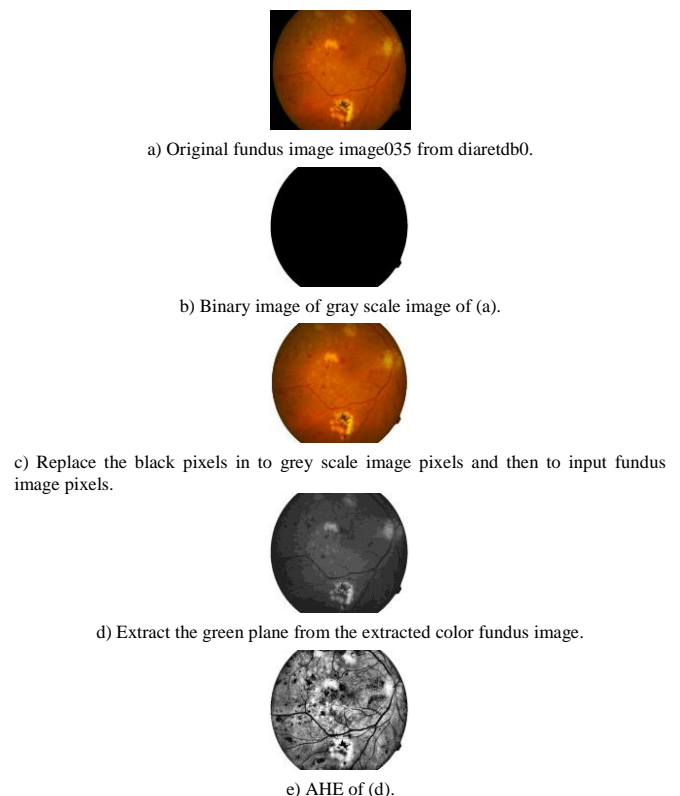


Figure 1. Preprocessing.

The paper [14 and 15] uses green plane of fundus

image for pre-processing, the dark region has the highest contrast against the background. Contrast enhancement using histogram equalization was implemented to improve the medical images enabling proper analysis and better visual perception of the disease [25]. Equalizing the images with black background increased the darkness within the details of the image. Fundus images are virtually red in color with black background where the black background does not have any details about the fundus and can therefore be safely removed by threshold techniques.

Then the green plane was extracted from the extracted input image for further enhancement by the Adaptive Histogram Equalization (AHE) which allows detailed study of small region of interest in fundus image. AHE bringing out more detail from image also amplifies noise in some homogeneous regions. Richness of details in the enhanced image is analysed using entropy values. The above pre-processing procedure was adapted from [26], and greatly facilitated the detection process. The pre-processed fundus images which were used in the vessel extraction process are shown in Figure 1.

3.4. Proposed Methodology

The fundus image of DR could have bright lesions, dark lesions fragments, normal vessels and abnormal blood vessels. Several methods have been developed over several years for determining normal retinal vasculature. Abnormal blood vessels exhibiting neovascularization may be distinguished from normal ones by their twisted and complex structure is very difficult to recognise. The proposed methodology segments blood vessels using FCM clustering and detects neovascularization region on the basis of compactness classifier. And then classifies neovascularization using feature extracted from the detected region.

3.4.1. Segmentation by Fuzzy C-means Clustering

Image segmentation helps to detect the neovascularization present in DR fundus image. Unsupervised algorithms used for segmentation are fully automatic and partition the regions in the feature space with high density [7]. The clustering based segmentation process groups the clusters with the objects which are similar to them while the dissimilar ones are grouped with the objects which belong to the other clusters. Fuzzy C-means (FCM) algorithm is an unsupervised clustering, preferably suitable for medical image segmentation [6]. FCM allows pixels that belong to multiple clusters with varying degrees of membership [12] whereas K-means is also a same type of segmentation which forces the pixels to belong exclusively to one class. Previously, clustering method segmented the anatomical structures of fundus images i.e., vessels [16], optic disc [8, 24]. In this study, FCM

clustering was implemented to segment the normal with abnormal blood vessels in fundus images.

FCM clustering clusters similar objects into three clusters: first cluster, clusters black related pixels from AHE image segment blood vessels, neovascularization, hemorrhages and fovea regions; second cluster – clusters grey related pixels which segment the back retinal portion of fundus image; third cluster – clusters white related pixels which segment white background, optic disc exudates is shown in Figure 2.

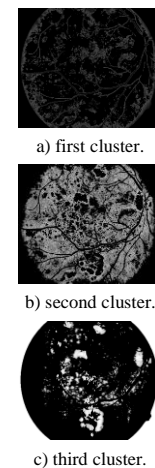


Figure 2. FCM clustering to segment DR fundus image with three clusters from AHE image Figure 1-e.

The main advantage of clustering based segmentation is that clustering does not have any predefined classes as in classification techniques. In the present study, the normal with abnormal blood vessels has been segmented directly and definitely.

3.4.2. Neovascularization Region Detection

Abnormal blood vessels are usually located at the junction of vasculature branches, but are not any different in colour or intensity from the dark lesions [15]. FCM clustering segments the neovascularization along with normal blood vessels. The compactness classifier Equation (1) becomes the basis for the demarcation of abnormal blood vessels from the first cluster.

$$Compactness = \frac{1}{4\pi l \frac{perimeter}{area}} \quad (1)$$

Multiple morphology dilation and erosion like morphology spur, morphological skel, morphology label, morphology area of the first cluster segmentation image assisted in bringing neovascularization blood vessels to the forefront receding other blood vessels and dark lesions to the background [15].

Neovascularization region was identified using a square window with 100×100 size based on two assumptions:

- a) When the square window is processed through the neovascularization region, it contains a greater

number of blood vessels (four or more) in comparison to the normal region.

b) When the square window is processed through the neovascularization region, it contains a greater area of blood vessels (more than 7% of the square window area) than the normal region.

Based on the above conventions, the square window uses a box to detect the neovascularization region, marking the region as shown in Figure 4. The regions manually marked by professional graders are shown in Figure 3. The sensitivity, specificity and accuracy are calculated for each marked image from Diaretdb0, Diaretdb1 and Messidor databases are tabulated in Tables 1, 2, and 3 respectively.

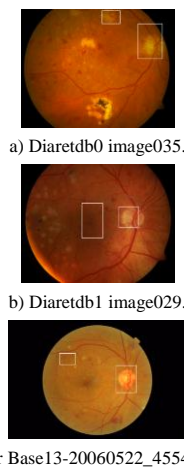


Figure 3. Manually marked neovascularization images by professional graders.

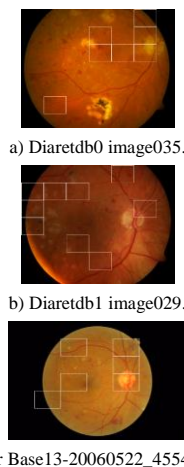


Figure 4. Neovascularization region detected using FCM on the basis of compactness classifier. The square window boxes indicate areas with neovascularisation.

Table 1. Neovascularization detection in diaretdb0 fundus images.

Images	TP	TN	FP	FN	Sen.	Spec.	Acc.
image031	0	251845	7790	2509	0.969996	0	0.960712
image032	867	239466	17053	4758	0.933521	0.154133	0.916798
image033	5625	242702	13817	0	0.946137	1	0.947292
image034	867	239466	17053	4758	0.933521	0.154133	0.916798
image035	4650	246142	10377	975	0.959547	0.826667	0.956696
image036	4650	246142	10377	975	0.959547	0.826667	0.956696
image037	3843	245335	11184	1782	0.956401	0.6832	0.950539
image038	3843	245335	11184	1782	0.956401	0.6832	0.950539
image039	3843	245335	11184	1782	0.956401	0.6832	0.950539
image040	3843	245335	11184	1782	0.956401	0.6832	0.950539
image041	3843	245335	11184	1782	0.956401	0.6832	0.950539
image042	3843	245335	11184	1782	0.956401	0.6832	0.950539
image043	3843	245335	11184	1782	0.956401	0.6832	0.950539
image044	3843	245335	11184	1782	0.956401	0.6832	0.950539
image045	3843	245335	11184	1782	0.956401	0.6832	0.950539
image046	3843	245335	11184	1782	0.956401	0.6832	0.950539
image047	3843	245335	11184	1782	0.956401	0.6832	0.950539
image048	0	249807	7656	4681	0.970264	0	0.952938
image049	0	241975	14848	5321	0.942186	0	0.923061
image050	4125	255826	693	1500	0.997298	0.733333	0.991634
Average (%)					95.6621	56.0507	94.8927

Table 2. Neovascularization detection in Diaretdb1 fundus images.

Images	TP	TN	FP	FN	Sen.	Spec.	Acc.
image016	600	246825	9694	5025	0.962209	0.106667	0.943851
image026	1983	239645	16874	3642	0.934219	0.352533	0.921738
image027	1983	239645	16874	3642	0.934219	0.352533	0.921738
image028	1983	239645	16874	3642	0.934219	0.352533	0.921738
image029	588	241043	15476	5037	0.939669	0.104533	0.921749
Average (%)					94.09	.25.37	.92.6163

Table 3. Neovascularization detection in Messidor fundus images.

Images	TP	TN	FP	FN	Sen.	Spec.	Acc.
20051020_44843_	0	247787	8733	5624	0.965	0	0.945
20051020_45110_	1392	245188	13016	2548	0.949	0.353	0.940
20051020_45137_	1392	245188	13016	2548	0.949	0.353	0.940
20051020_62709_	1392	245188	13016	2548	0.949	0.353	0.940
20051020_62802_	1392	245188	13016	2548	0.949	0.353	0.940
20051214_52492_	4047	244025	12500	1572	0.951	0.720	0.946
20060522_45541_	4275	251979	4540	1350	0.982	0.76	0.977
20060522_45583_	4275	251979	4540	1350	0.982	0.76	0.977
20051208_42314_	3225	240456	16588	1875	0.935	0.632	0.929
Average (%)					95.67	47.6	94.82

These above 34 images were used in our experiment to map the exact location of neovascularization for each image achieves an overall accuracy in detection accuracy 94.5531% with sensitivity 95.4489% and specificity 49.308% respectively. The Receiver Operator Curve (ROC) was plotted with true positive rate (sensitivity) as the vertical axis, against the false positive rate (100–specificity) as the horizontal axis on different pixels. ROC graph is plotted to show the performance of neovascularization detected pixels Figure 5.

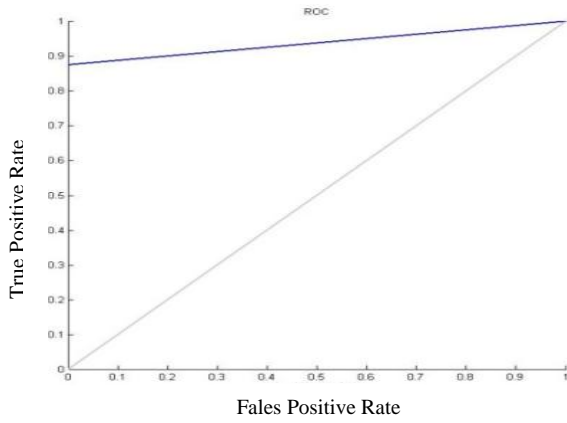


Figure 5. ROC curve of the pixels in neovascularization detected region using proposed methodology with the pixels presented in the same region in manually marked region.

Regions with large number of compactness representative of abnormal blood vessels were selected from the neovascularization detected region. Pixels in neovascularization detected region using the proposed methodology were compared with pixels manually marked in the same region. From the ROC plot it is evident that the images has been correctly segmented the abnormal blood vessels from images.

Manual observation and professional graders annotation mentioned in section 3.2 is invaluable in detection of the neovascularization region. A word of caution-there is every likelihood of marking non-neovascularization vessels as neovascularization vessels Figures 4-a, 4-b, and 4-c, because of the presence of minute normal blood vessels and hemorrhages. Awareness of this possibility is essential to avoid misdetection and misinterpretation of findings. Accuracy of judgement is imperative to ensure proper follow-up.

3.4.3. Feature Extraction

Strategic extraction of features from the selected region is significant for accurate classification of neovascularization region. The following 11 features are used to illustrate the neovascularization from each detected region.

- *Number of Segments*: the segments calculated through the compactness classification Equation (1).
- *Gradient variation*: Standard deviation for the segment is calculated using Sobel gradient. This feature is based on the more contrast variation of abnormal vessels than the normal vessels.
- *Mean*: Average value of all the elements in the matrix i.e., pixels in an image, formulated as Equation (2)

$$Mean = \mu = \frac{1}{N} \sum_{i=1}^m \sum_{j=1}^n P(i, j) \quad (2)$$

where, N is the number of pixels in the image, i and j -values of row and column of the image, m and n -final

values of the row and column of the image, $P(i, j)$ is a matrix of the image.

- *Variance*: Variance is a measure of deviation of gray levels in an image from the mean calculated by Equation (3).

$$Variance = \sum_{i=0}^m \sum_{j=0}^n (i - \mu)^2 P(i, j) \quad (3)$$

- *Standard Deviation*: Standard deviation (σ) is the square root of the variance of elements in the matrix by using Equation (4).

$$\sigma = \sqrt{\frac{1}{N-1} \sum_{i=1}^m \sum_{j=1}^n (p(i, j) - \mu)^2} \quad (4)$$

- *Contrast*: Contrast is a measure of the local intensity level variation which gives higher value for high contrast image. It is given by Equation (5).

$$Contr = \sum_{i=0}^m \sum_{j=0}^n (i - j)^2 P(i, j) \quad (5)$$

- *Correlation*: Correlation calculates the linear dependency of the gray level values between the pixels at the specified positions related to each other is calculated by Equation (6).

$$Corrm = \frac{\sum_{i=0}^m \sum_{j=0}^n (i - \mu)(j - \mu)P(i, j)}{\sigma^2} \quad (6)$$

- *Entropy*: The entropy of a retinal image can be defined as a measure of the uncertainty associated with a random variable. Homogeneous regions have high entropy calculated using Equation (7).

$$Entro = -\sum_{i=0}^m \sum_{j=0}^n p[i, j] \log_2(p[i, j]) \quad (7)$$

- *Energy*: Angular second moment is also known as Energy. It is the sum of squares of entries in the Gray-Level Co-occurrence Matrix. This measures the image homogeneity and is high when pixels are very similar formulated as Equation (8).

$$Energy = \sum_{i=0}^m \sum_{j=0}^n (p[i, j])^2 \quad (8)$$

- *Homogeneity*: Homogeneity can measure the closeness of the distribution of elements in the GLCM to the GLCM diagonal represented by Equation (9).

$$Homom = \sum_{i=0}^m \sum_{j=0}^n \frac{1}{1 + (i - j)^2} P(i, j) \quad (9)$$

- *Cluster Shade*: Cluster shade reduces the number of operations in terms of the pixel values contained in a given $M \times N$ neighborhood containing gray levels by Equation (10).

$$Cshad = \sum_{i=0}^m \sum_{j=0}^n \{i + j - \mu_x - \mu_y\}^3 P(i, j) \quad (10)$$

3.4.4. Classification

Neural networks provide methodology for resolving highly non-linear problems on the basis of classification. In the research work, FFBN was selected for classification to avoid the misdetection of neovascularization in FCM clustering, because of its prompt training phase and good classification performance, with accompanying feedback mechanism. The features extracted values fed as input to the FFBN for each region to be classified as neovascularization. Each value from the input layer is replicated and sent to all the hidden neurons in the fully interconnected structure. The output layer transcribes the hidden layer activations into a scale where a value less than 1.5 signifies neovascularization region and a value greater than 1.5 indicates non-neovascularization region.

Neovascularization classification using FFBN achieves maximum accuracy of 84% with sensitivity of 31% and specificity of 94% respectively.

Previously [14], neovascularization classification using SVM classifier with 15 features achieved an accuracy range of 82%. In the present method, neovascularization classified using FFBN with 11 features, achieving a fine accuracy range of 84%. The proposed approach is developed by using MATLAB R2014a code with Window7 Ultimate 32-bit Operating System, powered by Intel(R) Core(TM) 2 Duo CPU T6600 @ 2.20GHz Processor and 3.00 GB RAM.

Processing time for the previous work [14] took less than one second per image classification and the classifier training phase took 2 min. For this work, neovascularization region detection of an image took approximately 0.3856seconds for the detection. The training phase for FFBN classification acquired 1.5 minutes, but this only has to be performed once prior in the system.

3.5. Performance in Real-Time Images

In clinics, IVFA images are used to treat the neovascularization in patients. Specialists examine the patients by injecting fluorescent dye into the blood vessels which flow through both normal and abnormal blood vessels of the eye helps in laser treatment. This fluorescent dye injection is harmful and causes discomfort to the patient. Automatic detection of abnormality greatly helps specialists. In this alternate methodology, the clinical specialist's free hand marking, of the neovascularization region is marked through Photoshop application and then performances have been calculated by comparing with the markings.

The sample neovascularization marked and classified clinic images are shown in Figure 6.

Confident performance measure achieves in detection using Bejan Singh eye hospital images maximum accuracy of 95.66% with sensitivity of 97.11% and specificity of 29% respectively, and by

Vasan eye care achieves maximum accuracy of 90.98% with sensitivity of 91.34% and specificity of 72.65% respectively. This measure can be providing confident in the detection of Neovascularization in the future DR analysis system.

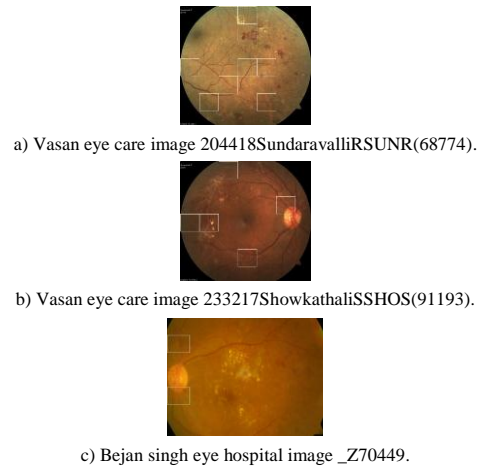


Figure 6. Neovascularization marked in hospital eye clinic images.

4. Discussion and Conclusion

Due to its severity, macular edema in NPDR and neovascularization in PDR can be treated only by laser [31]. All the other abnormalities in NPDR can be mended by drugs through controlling the glucose level of the patient. Neovascularization in PDR is the most serious among all DR conditions. It is also the rarest.

Neovascularization in PDR cannot be reverted because the abnormal blood vessels are interconnected with the normal blood vessels and interrupt the regular blood flow to the eye. These abnormal blood vessels need to be sealed only through laser treatment in order to uphold the normal flow of blood towards the normal vessels [31].

The paucity of research in the area of neovascularization detection is due to the lower percentages of reported cases. Neovascularization is receiving a lot of attention today because of its severity. Developing an automated system to find the abnormalities might reduce the cost of screening.

Patients have to rely on the expertise of ophthalmologists rather than trust screening systems because of the limitations of the latter. The challenges in the management of neovascularization are firstly, its severity, and secondly, the difficulty in accurate identification of abnormal blood vessels because of their resemblance to normal blood vessels. Automation of the detection procedure is rendered doubly difficult because of the similarity between normal and neovascularization regions.

Professional graders do not favour the system of marking regions with each and every line of neovascularization vessels prior to treatment.

Detecting and confirming one single region as a neovascularization region suffices to adopt treatment

measures, because sealing of the abnormal blood vessels is not done on an individual basis. The entire retina is subjected to treatment when professional graders confirm the presence of neovascularization in the eye. However, the present approach would be helpful to professional graders as a confidence-building measure because of the high accuracy levels attained (84% in classification process). Section 3.1 mentions the variation in size of neovascularization fundus images available in databases. The module developed during the present study is therefore adaptable and wide in scope, in addition to being able to handle varying image resolutions present in different clinical images. The proposed methodology yields encouraging results for future development.

This paper has validated an automated system which enables detection and classification of neovascularization vasculature in both NVD and NVE of DR images. The proposed methodology can also be used to state whether the patient is in a high-risk group or not. High risk PDR neovascularization is defined as any one of the following categories: NVD $>1/3$ disc area, NVD with vitreous hemorrhage, NVE $\geq 1/2$ disc area with vitreous hemorrhages [13].

Neovascularization with high-risk characteristics need prompt laser treatment, thereby necessitating accurate and faultless detection and identification of neovascularization to save the patient's eyesight.

There are a large number of areas can be worked as further investigations, as like detecting abnormal blood vessels in the optic disc region competently will be helpful for ophthalmologists to provide laser treatment.

High-risk characteristics identification might help doctors to treat patients excellently. The proposed methodology could go a long way in reducing the burden on manual graders for the purpose of analyzing serious DR abnormalities.

Acknowledgement

The authors would like to thank Dr.M.Pratap, Ophthalmologist of Vasan Eye Care, Nagercoil, India and Dr.S.M.BejanSingh, Ophthalmologist, BejanSingh Eye Hospital, Nagercoil, India for help in collecting the images.

References

- [1] Abràmoff M., Garvin M., and Sonka M., "Retinal Imaging and Image Analysis," *IEEE Reviews in Biomedical Engineering*, vol. 3, pp. 169-208, 2010.
- [2] Akila T. and Kavitha G., "Detection and Classification of Hard Exudates in Human Retinal Fundus Images Using Clustering and Random Forest Methods," *International Journal of Emerging Technology and Advanced Engineering*, vol. 4, no. 2, pp. 24-29, 2014.
- [3] Belhadi S. and Benblidia N., "Automated Retinal Vessel Segmentation using Entropic Thresholding Based Spatial Correlation Histogram of Gray Level Images," *The International Arab Journal of Information Technology*, vol. 12, no. 5, pp. 441-447, 2015.
- [4] Boyd K. and Janigian R., "What is Diabetic Retinopathy," *Eye Smart*, Eye health information from the American Academy of Ophthalmology, The Eye M.D Association, Prohibited by US and international copyright law, 2013.
- [5] Cheriyan J., Menon H., and Narayanankutty K., "3D Reconstruction of Human Retina from Fundus Image-A Survey," *International Journal of Modern Engineering Research*, vol. 2, no. 5, pp. 3089-3092, 2012.
- [6] Christ J. and Parvathi R., "Fuzzy C-Means Algorithm for Medical Image Segmentation," in *Proceedings of 3rd International Conference on Electronics Computer Technology*, Kanyakumari, pp. 33-36, 2011.
- [7] Christ J. and Parvathi R., "Segmentation of Medical Image using Clustering and Watershed Algorithms," *American Journal of Applied Sciences*, vol. 8, no. 12, pp. 1349-1352, 2011.
- [8] Devasia T., Jacob P., and Thomas T., "Automatic Optic Disc Boundary Extraction from Color Fundus Images," *International Journal of Advanced Computer Science and Applications*, vol. 5, no. 7, pp. 117-124, 2014.
- [9] DIARETDB0 database. Available online: <http://www2.it.lut.fi/project/imageret/diaretdb0/>, Last Visited, 2007.
- [10] DIARETDB1 database. Available online: <http://www2.it.lut.fi/project/imageret/diaretdb1/>, Last Visited, 2007.
- [11] Fleming A., Philip S., Goatman K., Olson J., and Sharp P., "Automated Microaneurysm Detection using Local Contrast Normalization and Local Vessel Detection," *IEEE Transactions on Medical Imaging*, vol. 25, no. 9, pp. 1223-1232, 2006.
- [12] Funmilola A., Oke O., Adedeji T., Alade O., and Adewusi E., "Fuzzy k-c-means Clustering Algorithm for Medical Image Segmentation," *Journal of Information Engineering and Applications*, vol. 2, no. 6, pp. 21-32, 2012.
- [13] Gerstenblith A. and Rabinowitz M., *The Wills Eye Manual, Office and Emergency Room Diagnosis and Treatment of Eye Disease*, Williams and Wilkins, 2012.
- [14] Goatman K., Fleming A., Philip S., Williams G., Olson J., and Sharp P., "Detection of New Vessels on the Optic Disc Using Retinal Photographs," *IEEE Transactions on Medical Imaging*, vol. 30, no. 4, pp. 972-979, 2011.
- [15] Hassan S., Bong D., and Premsenthil M., "Detection of Neovascularization in Diabetic

- Retinopathy,” *Journal Digit Imaging*, vol. 25, no. 3, pp. 437-444, 2011.
- [16] Kande G., Savithri S., and Subbaiah P., “Segmentation of Vessels in Fundus Images using Spatially Weighted Fuzzy C-Means Clustering Algorithm,” *International Journal of Computer Science and Network Security*, vol. 7, no. 12, pp. 102-109, 2007.
- [17] Manimala K. and Gokulakrishnan K., “Detection of Microaneurysms in Color Fundus Images,” *International Journal of Emerging Technology and Advanced Engineering*, vol. 4, no. 2, pp. 30-37, 2014.
- [18] MESSIDOR database. Available online: <http://messidor.crihan.fr/>, Last Visited, 2004.
- [19] Nandy M., Mandal A., Banerjee S., and Ray K., “A Prescription Survey in Diabetes Assessing Metformin use in a Tertiary Care Hospital in Eastern India,” *Journal of Pharmacology and Pharmacotherapeutics*, vol. 3, no. 3, pp. 273-275, 2012.
- [20] Niemeijer M., Abràmoff M., and Ginneken B., “Information Fusion for Diabetic Retinopathy CAD in Digital Color Fundus Photographs,” *IEEE Transactions on Medical Imaging*, vol. 28, no. 5, pp. 775-785, 2009.
- [21] Niemeijer M., Ginneken B., Staal J., Suttorp M., and Abràmoff M., “Automatic Detection of Red Lesions in Digital Color Fundus Photographs,” *IEEE Transactions on Medical Imaging*, vol. 24, no. 5, pp. 584-592, 2005.
- [22] Niemeijer M., Ginneken B., Cree M., Mizutani A., Quéllec G., Sánchez C., Zhang B., Hornero R., Lamard M., Muramatsu C., Wu X., Cazuguel G., You J., Mayo A., Li Q., Hatanaka Y., Cochener B., Roux C., Karray F., García M., Fujita H., and Abràmoff M., “Retinopathy Online Challenge: Automatic Detection of Microaneurysms in Digital Color Fundus Photographs,” *IEEE Transactions on Medical Imaging*, vol. 29, no. 1, pp. 185-195, 2010.
- [23] Osareh A., Mirmehdi M., Thomas B., and Markham R., “Automated Identification of Diabetic Retinal Exudates in Digital Colour Images,” *British Journal of Ophthalmology*, vol. 87, no. 10, pp. 1220-1223, 2003.
- [24] Padmanaban K. and Jagadeeshkannan R., “Localization of Optic Disc Using Fuzzy C Means Clustering,” *International Conference on Current Trends in Engineering and Technology*, Coimbatore, pp. 571-573, 2013.
- [25] Raju A., Dwarakish G., and Reddy V., “A Comparative Analysis of Histogram Equalization based Techniques for Contrast Enhancement and Brightness Preserving,” *International Journal of Signal Processing, Image Processing and Pattern Recognition*, vol. 6, no. 5, pp. 353-366, 2013.
- [26] Suma K. and Kavitha V., “Histogram Equalization based methods for Fundus Images: A Survey,” in *Proceedings of National Conference on Computing and Communication*, pp. 206-210, 2015.
- [27] Thacker T., “India has Largest Number of Diabetes Patients,” Report, 2009.
- [28] Thomas N., Mahesh T., and Shunmuganathan K., “Detection and Classification of Exudates in Diabetic Retinopathy,” *International Journal of Advance Research in Computer Science and Management Studies*, vol. 2, no. 9, pp. 296-305, 2014.
- [29] Vimala A. and Mohideen K., “An Efficient Approach for Detection of Exudates in Diabetic Retinopathy Images Using Clustering Algorithm,” *Journal of Computer Engineering*, vol. 2, no. 5, pp. 43-48, 2012.
- [30] Vislislis J. and Oetting T., “Diabetic Retinopathy: from One Medical Student to Another”, *EyeRounds.org*, 2010.
- [31] Viswanath K. and McGavin M., “Diabetic Retinopathy: Clinical Findings and Management-Review Article,” *Community Eye Health*, vol. 16, no. 46, pp. 21-24, 2003.
- [32] Walter T., Klein J., Massin P., and Erginay A., “A Contribution of Image Processing to the Diagnosis of Diabetic Retinopathy-Detection of Exudates in Color Fundus Images of the Human Retina,” *IEEE Transactions on Medical Imaging*, vol. 21, no. 10, pp. 1236-1243, 2002.



Suma Gandhimathi received B.E., degree in Computer Science and Engineering in 2009, SMEC, Chennai affiliated to Anna University: Chennai. She has received M.E., degree in Computer Science and Engineering in 2012, Muthayammal Engineering College, Rasipuram affiliated to Anna University: Chennai. She is the University Rank Holder in PG. She is currently working toward the Ph.D., degree in Computer Science and Engineering in Anna University: Chennai. Her area of research interest is Medical Image Processing.



Kavitha Pillai received her B.E degree in Computer Science and Engineering in 1996 from MS University and M.E degree in Computer Science and Engineering in 2000 from Madurai Kamaraj University. She is the University Rank Holder in UG and Gold Medalist in PG. She received Ph.D., degree in Computer Science and Engineering from Anna University Chennai in 2009. Right from 1996 she is in the Department of Computer Science & Engineering under various designations. Presently she is working as Associate Professor in the Department of CSE at University College of Engineering Kanchipuram, Anna University. Currently, under her guidance ten Research Scholars are pursuing Ph.D., as full time and part time. Her research interests are Wireless networks, Mobile Computing, Network Security, Wireless Sensor Networks, Image Processing, and Cloud Computing. She has published many papers in Conference, National and International journal in areas such as Network security, Mobile Computing, wireless network security, and Cloud Computing. She is a life time member of ISTE.